*Pure Appl. Chem.*, Vol. 74, No. 3, pp. 475–481, 2002.


# Superhard nanocomposite coatings. From basic science toward industrialization*

S. Veprek[1,‡] and M. Jilek[2,§]

*[1]Institute for Chemistry of Inorganic Materials, Technical University Munich, Lichtenbergstrasse 4, D-85747 Garching, Germany; [2]SHM, Ltd., Novy Malin 266, CZ-788 03 Novy Malin, Czech Republic*

*Abstract*: A variety of superhard coatings with Vickers plastic hardness exceeding 40 GPa have been reported by several research groups during the last five years (for recent reviews see refs [1,2]). However, one has to distinguish between superhard nanocomposites, such as nc-TiN/a-$Si_3N_4$, nc-TiN/a-$Si_3N_4$/a- and nc-$TiSi_2$, nc-$(Ti_{1-x}Al_x)N$/a-$Si_3N_4$, nc-TiN/$TiB_2$, nc-TiN/BN, etc. where the high hardness originates from the nanostrucutre and, therefore, remains stable upon annealing to high temperatures [1], and coatings, such as CrN/Ni, ZrN/Ni, and others [2] in which the measured high hardness is due to a high compressive stress that is induced in the coatings due to energetic ion bombardment during their deposition (e.g., by magnetron sputtering). We also summarize the recent progress in the industrial applications of the superhard nanocomposite coatings on machining tools.

## INTRODUCTION

There are many examples which show that compressive stress in the coatings [1] or in a bulk material [3] results in an apparent increase of the plastic hardness measured by the load-depth sensing indentation technique. In the case of relatively soft ductile material that showed pile-up during the indentation, this apparent enhancement of the measured hardness is an artifact of that technique because no change of the hardness was found when the hardness was evaluated from the projected area of the remaining plastic deformation [3]. Because of the pile-up, the load-depth sensing technique underestimates the indentation depth and consequently overestimates the values of hardness and elastic modulus [3].

A strong enhancement of the hardness due to a high biaxial compressive stress in the coatings was reported, e.g., for $HfB_2$ (70 GPa) [4], (TiAlV)N, TiN (100 GPa and 80 GPa, respectively [5]), and $TiB_2$ (68 GPa [6]). However, when the coatings were annealed at ≥400 °C, the stress decreased below 2 GPa and the hardness decreased to the value of bulk materials (34 GPa for $TiB_2$ and ≤20 GPa for the others). Obviously, the enhancement of the hardness due to high compressive stress is of little interest for applications, such as cutting tools for dry machining where the coatings reach a high temperature of 600–800 °C.

Our recent studies showed that for the ZrN/Ni and CrN/Ni coatings (for their preparation see [2]) whose high hardness of ≥40 GPa is solely due to a high compressive stress of ≥5 GPa, as well as for superhard nanocomposites, such as nc-TiN/a-$Si_3N_4$ and nc-$(Ti_{1-x}Al_x)N$/a-$Si_3N_4$ with either a high (≥5 GPa) or low (≤1 GPa) compressive stress, the values of plastic hardness measured by the load-depth sensing indentation technique agree fairly well with the Vickers hardness evaluated from the projected area of the remaining plastic deformation [8]. Also, the hardness values of a variety of superhard

*Lecture presented at the 15th International Symposium on Plasma Chemistry, Orléans, France, 9–13 July 2001. Other presentations are presented in this issue, pp. 317–492.

‡Corresponding author: E-mail: veprek@ch.tum.de

§E-mail: shm@shm-cz.cz

nanocomposites measured by the load-depth sensing technique at sufficiently large loads of 50 to 200 mN (in the case of 15–20-μm-thick coatings even up to 1000 mN) agree fairly well with the Vickers hardness calculated from the projected area of the plastic deformation within the broad range of hardness between 20 and 100 GPa [9]. These nanocomposites were deposited by plasma CVD and, therefore, have a low compressive stress of ≤1 GPa. It can be concluded that the very high values of the plastic hardness of these nanocomposites were carefully checked and can be considered as correct.

All the superhard nanocomposites are deposited by means of plasma induced processing, such as plasma-induced CVD [1,9–11,17–18] and PVD including magnetron sputtering [6,12,13] and vacuum arc evaporation [14]. Alternatively, combined plasma PVD and CVD are used in which the metals (Ti, Al, ...) are evaporated either by means of vacuum arc [14,15] or by sputtering [16] and the nonmetals are introduced as gaseous reactants (e.g., $SiH_4$, $BCl_3$, $B_3N_3H_6$). Voevodin *et al.* used pulsed laser ablation for the deposition of hard wear resistant nanocomposite coatings (see [19] and references therein). We refer to these papers for further details.

## GENERIC DESIGN CONCEPT AND THERMAL STABILITY OF SUPERHARD NANOCOMPOSITES

The superhard nanocomposites are prepared according to the generic design principle [10] that is based on a strong spinodal decomposition, which results in a formation of a nanostructure. The thermodynamic criterion for spinodal decomposition to occur is negative second derivative of the Gibbs free energy of the mixed phase (e.g., $Ti_xSi_yN_z$) with a change of the composition (e.g., toward $TiN + Si_3N_4$). It means that any spontaneous infinitesimal, local fluctuation of the composition of the mixed phase leads to a decrease of the Gibbs free energy of the system. Consequently, the phase segregation occurs spontaneously without any need for nucleation of either phase. In such a way, a nanocomposite is formed by a self-organization with a characteristic length scale (crystallite size), which is determined by the balance between the decrease of the Gibbs free energy due to phase segregation, chemical gradients, and incoherency strain at the interface. When formed, such nanocomposites are stable against coarsening within the temperature range where the second derivative of the Gibbs free energy of the segregated system remains negative. Thus, an appropriate selection of binary or ternary refractory hard materials allows one to prepare superhard nanocomposites whose nanostructure and the resultant hardness remain stable up to high temperatures of 1100 °C. For further details, we refer to [9–11].

In these nanocomposites, the nanocrystals of the transition metal nitride are imbedded within about 1 monolayer thin amorphous tissue which provides the materials with a high hardness, resistance against crack formation and propagation and a high thermal stability up to 1100 °C (see [1,9–11,14,17,18] and references therein). Examples of such systems are nc-$M_nN$/a-$Si_3N_4$ {M = Ti, W, V, $(Ti_{1-x}Al_x)N$/a-$Si_3N_4$ [1,17,18] and other hard transition-metal nitrides}, TiN/$TiB_2$ [1,6,12,13], nc-TiN/BN [20] and others (see review [1]). In the case of the nc-TiN/a-$Si_3N_4$, nc-$(Ti_{1-x}Al_x)N$/a-$Si_3N_4$, nc-TiN/a-$Si_3N_4$/a-$TiSi_2$, and TiN/$TiB_2$ it was shown that the hardness, measured after the annealing at room temperature, remains unchanged up to the recrystalization temperature of 900–1100 °C. The highest recrystallization temperature is achieved for nanocomposites with the optimal $Si_3N_4$ content corresponding to the percolation and lowest crystallite size of about 3 nm. Figure 1 shows a typical example of the thermal stability of such superhard nanocomposites (see [1,9,11]). This is an unambiguous evidence that the superhardness is due to the nanostructure.

Another evidence of the superhardness being due to the formation of the nanostructure is the spontaneous formation of the nanocomposite due to self-organization as discussed in our earlier papers [1,10,11,22]. For example, Hammer *et al*. deposited amorphous Ti-B-N films by magnetron sputtering at room temperature with a hardness between 27 and 29 GPa, depending on the composition. Upon annealing to ≥600 °C, a nanocomposite structure was formed and the hardness increase to about 40 GPa [13]. Other examples of such selforganization and hardness increase can be found in the work of Andrievski *et al*. [23,24] (see discussion in [1]).

In many cases reported in the literature, the high measured hardness was attributed to "nanocomposites", although it was predominantly or solely due to the high biaxial compressive stress. For example, Musil *et al*. reported superhardness of ≥40 GPa for a series of coatings consisting of hard transition-metal nitride (e.g., ZrN, CrN) and a soft metal that does not form nitride (e.g., Ni, Cu) (see [2] and references therein). More recently, it was shown that the high hardness of these coatings is due predominantly to the high biaxial compressive stress induced in the coatings during their deposition by means of unbalanced magnetron sputtering [21].

The high hardness strongly decreases to the ordinary value for the bulk material of ≤20 GPa upon annealing to ≥400 °C when the stress relaxes as shown in Fig. 2 [21].

The experimental data available so far strongly suggest that the reported superhardness in these coatings (called also "nanocomposites") is a simple consequence of the high biaxial stress in a similar way as reported for $HfB_2$, (TiAlV)N, TiN, and $TiB_2$ mentioned above. No effect of the nanostructure on the reported enhancement of the superhardness could be found because no changes of the microstrusture occured upon the annealing. We refer to [21] for further details.

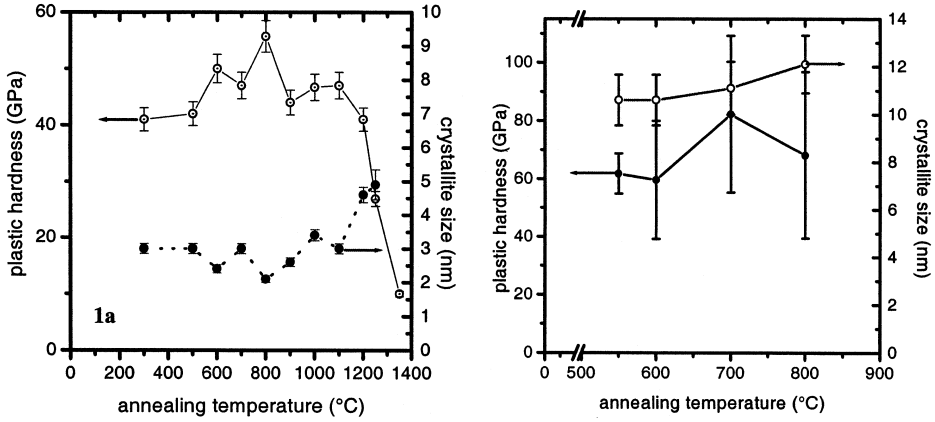


**Fig. 1** (a) Example of annealing behavior of a $(Ti_{1-x}Al_x)N/a\text{-}Si_3N_4$ sample deposited on cemented carbide substrate at a temperature of about 300 °C; (b) ternary nc-TiN/a-$Si_3N_4$/a-$TiSi_2$ nanocomposite deposited on steel substrate; total Si-content 8 at. %, 3.5 % $Si_3N_4$, 4.1 % $TiSi_x$, thickness of the coating 20 μm.

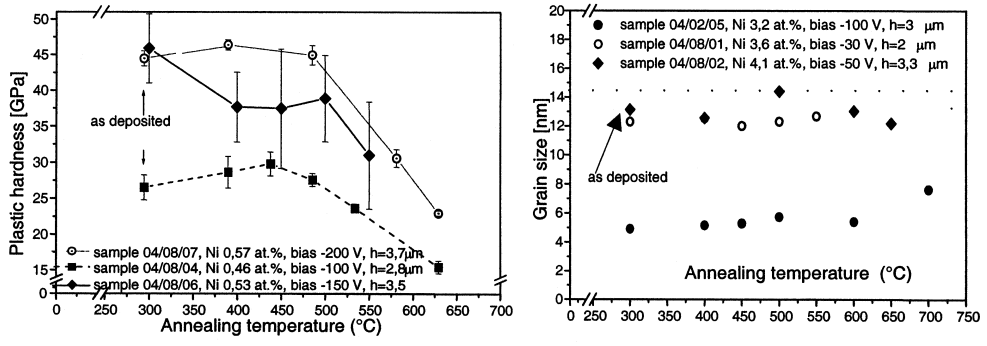


**Fig. 2** (a) Decrease of the hardness and (b) no change of the crystallite size is observe upon annealing of the ZrN/Ni coatings above 400 °C. Simultaneously, a decrease of the high compressive stress in the coatings is observed (see [21]).

An interesting question is also the extent of the hardness enhancement due to the formation of a nanostructure and to compressive stress in the TiN-$TiB_2$ coatings prepared by magnetron sputtering at low pressure The data reported in [6] showed an enhancement of the hardness to about 68 GPa for pure $TiB_2$ (bulk value of 34 GPa [25]) due to the compressive stress and its decrease to ≤55 GPa for Ti-B-N nanocomposites with nitrogen content of 25–30 at. % [6]. With reference to the above mentioned results of Hammer *et al*. regarding hardness increase up to about 40 GPa upon annealing of such films deposited at room temperature one would expect that the high hardness of 55 GPa reported in [6] is due partially to the formation of nanostructure and to the high compressive stress. A lack of changes of the crystallite size upon annealing of these films is not any guarantee of the stability of their hardness, because it does not reflect the relaxation of the compressive stress, as shown in Fig. 2. Therefore, more detailed studies of this system are needed.

## MECHANICAL PROPERTIES OF THE SUPERHARD NANOCOMPOSITES

Conventional hard materials are brittle and undergo fracture at a strain of ≤0.1 % [25]. It was therefore surprising to find in the nanocomposites an unusual combination of very high hardness of 40–100 GPa, high elastic recovery of 80–94 %, and a high resistance against crack formation [10,17,25]. A recent theoretical analysis of the experimental data [22] showed that they can be understood in terms of the conventional fracture physics and mechanics when this is scaled down to a crystallite size of 3–5 nm. As already shown in our earlier papers, the superhardness is a simple consequence of the formation of stable nanocomposites with a strong interface which avoids grain boundary sliding [10]. The high resistance against crack formation is due to the small stress concentration factor of 2–4 in the nanocomposites, which is orders of magnitude smaller than that of ordinary microcrystalline materials. For the same reasons, the yield stress needed to propagate a nanocrack is much higher in the nanocomposite than in a microcrystalline material even if they have the same stress intensity factor [22]. The high elastic recovery of up to 94 % and high range of predominantly elastic deformation of ≥10 % which results in a very high elastic energy density upon indentation can be understood in terms of reversible flexing. The very high elastic modulus as measured by the indentation technique is due most probably the high pressure under the indenter. For space limitations here we refer to [22] for further details.

## INDUSTRIAL APPLICATIONS

The industrial-scale coating technology by means of vacuum arc evaporation from a central cathode consisting of segments of the different metals was developed for the superhard nc-$(Ti_{1-x}Al_x)N$/a-$Si_3N_4$ coatings and is now available for a large-scale production [14]. The coatings show a significantly improved cutting performance as compared with the conventional ones. Figure 3 shows schematics of the equipment. It consist of a central cathode with two segments made of titanium and an aluminium/silicon eutectic alloy. The movement of the cathode spot of the arc is controlled by magnetic field, which is induced by a combination of permanent magnets and electric coils. The axial component of the field drives the motion of the spot around the axis of symmetry, whereas the axial shift of the magnetic field, which is controlled by the coils, determines the fraction of the duty time of the cathodic spots on the individual segments. This spot is moved at a time scale of several tens of millisecond per segment, which assures atomic mixing of the metallic components during the deposition on tools. The latter are mounted on the substrate holders, which are fixed in an axially symmetric manner and rotate along their own axes. The typical deposition conditions are: substrate temperature: 550 °C; substrate bias 200 V; total pressure 0.2 Pa; arc voltage 32 V; arc current 100 A; substrate bias 200 V; substrate current 6 A [14]. Meanwhile, the arrangement of the central cathode and the control of the movement of the cathodic spot were further developed and improved, which resulted in a significant decrease of the emission of the macroparticles and a much better smoothness of the surface, which in turn led to a further improvement of the cutting performance of the coated tools.

A variety of tools for dry and fast turning, milling, drilling are coated and successfully used by the customers. Under the conditions of the dry machining, which saves the environmentally risky coolants and saves costs, the temperature of the cutting edge and of the rake reaches 600–800 °C. This illustrates the need of thermally stable and oxidation resistant coatings.

Figure 4 shows an example of the performance of the recently developed superhard nanocomposite coating nc-$(Ti_{1-x}Al_x)N$/a-$Si_3N_4$ in comparison with the conventional TiN and $(Ti_{1-x}Al_x)N$ coatings in dry milling at a relatively high cutting speed.

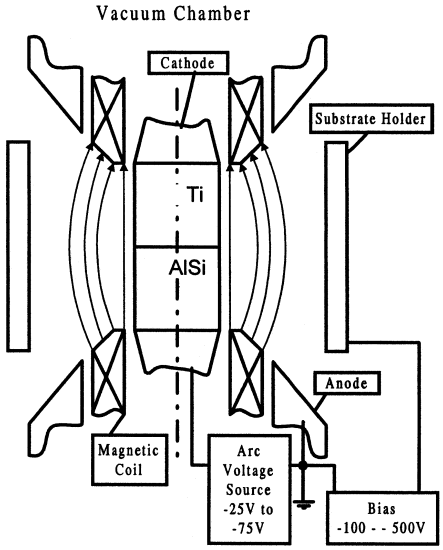


**Fig. 3** Schematics of the industrial coating equipment based on vacuum arc evaporation from segmented central cathode consisting of titanium and aluminium/silicon eutectic alloy. The movement of the cathode spot is controlled by magnetic field, which is induced by a combination of permanent magnets and electrical coils (see text).

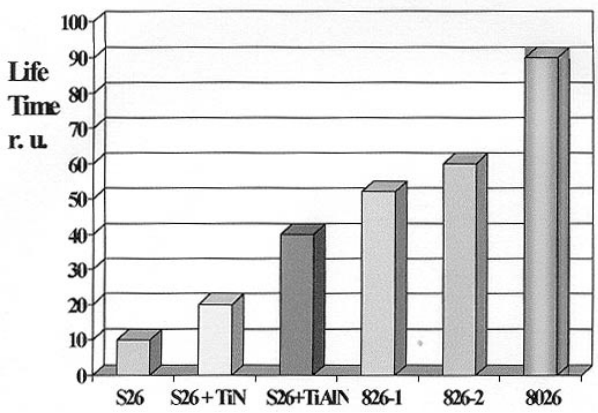


**Fig. 4** Example of the cutting performance of various coatings. Symmetric milling of steel CK45, feed 0.23 mm/tooth, depth of cut 2 mm, cutting speed 179 m/min. The meaning of the symbols: S26 indexable insert SPCN 1203EDSR (P20-P30) without any coating, S26+TiN TiN-coated, S26+TiAlN (TiAl)N-coated, 826-1 and 826-2 the same insert coated with nc-$(Ti_{1-x}Al_x)N$/a-$Si_3N_4$ nanocomposite of the 1st and 2nd generation, respectively, 8026 nc-$(Ti_{1-x}Al_x)N$/a-$Si_3N_4$ multilayer nanocomposite coatings 3rd generation 2000.

One can clearly see the progress in the development and improvement of these coatings. The performance of the indexable inserts coated with the 3rd generation of multilayer nc-$(Ti_{1-x}Al_x)N$/a-$Si_3N_4$ coatings MARWIN® MT is improved by a factor of 9 as compared to the uncoated tool and more than 2 as compared to the standard $(Ti_{1-x}Al_x)N$ coating.

## CONCLUSIONS

A significant increase of the hardness measured by the load-depth sensing indentation technique can be achieved either by a high biaxial compressive stress induced in the coatings by energetic ion bombardment during their deposition or by the formation of a stable nanostructure due to spinodal decomposition and phase segregation. Whereas in the former case, the hardness decreases upon annealing to ≥400 °C, the latter superhard coatings remain stable up to high temperatures of 1 100 °C. This is a significant advantage of these coatings in industrial applications, such as dry machining, where high temperatures are reached at the cutting edge of the tool.

## ACKNOWLEDGMENTS

We should like to thank company PRAMET Tools for performing the cutting tests and our coworkers and colleagues for their enthusiastic work and support. The present work was supported by the NATO Science for Peace Project number SfP 972379 and the German Science Foundation.

## REFERENCES

1. S. Veprek. *J. Vac. Sci. Technol. A* **17**, 2401 (1999).
2. J. Musil. *Surf. Coat. Technol.* **125**, 322 (2000).
3. T. Y. Tsui, W. C. Oliver, G. M. O. Pharr. *J. Mater. Res*. **11**, 752, 760 (1996).
4. W. Herr and E. Broszeit. *Surf. Coat. Technol*. **97**, 335 (1997).
5. J. Musil, S. Kadlec, J. Vyskocil, V. Valvoda. *Thin Solid Films* **167**, 107 (1988).
6. C. Mitterer, P. H. Mayhofer, M. Beschliesser, P. Losbichler, P. Warbichler, F. Hofer, P. N. Gibson, W. Gissler, H. Hruby, J. Musil, J. Vlcek. *Surf. Coat. Technol*. **120–121**, 405 (1999).
7. A. J. Perry, J. N. Matossian, S. J. Bull *et al*. *Surf. Coat. Technol*. **120–121**, 337 (1999).
8. S. Veprek, P. Karvankova, J. Prochazka, H. Männling, M. Jilek. *Mater. Res. Soc. Symp. Proceedings*, Vol. 697, MRS Fall Meeting, Boston, November 2001 (2002). In press.
9. H. Männling, D. S. Patil, K. Moto, M. Jilek, S. Veprek. *Surf. Coat. Technol.* **146–147**, 263 (2001).
10. S. Veprek and S. Reiprich. *Thin Solid Films* **268**, 64 (1996).
11. A. Niederhofer, T. Bolom, P. Nesladek, K. Moto, C. Eggs, D. S. Patil, S. Veprek. *Surf. Coat. Technol*. **146–147**, 183 (2001).
12. P. H. Mayhofer and C. Mitterer. *Surf. Coat. Technol*. **133–134**, 131 (2000).
13. P. Hammer, A. Steiner, R. Villa *et al*. *Surf. Coat. Technol*. **68–69**, 194 (1994).
14. P. Holubar, M. Jilek, M. Sima. Int. Conf. on Metallurgical Coatings and Thin Films, San Diego April 2000, *Surf. Coat. Technol*. **133–134**, 145 (2000).
15. S. Veprek, P. Nesladek, A. Niederhofer, F. Glatz, M. Jilek, M. Sima. *Surf. Coat. Technol*. **108–109**, 138 (1998).
16. J. Prochazka and S. Veprek. 2001. Unpublished results.
17. S. Veprek, M. Haussmann, S. Reiprich. *J. Vac. Sci. Technol. A* **14**, 46 (1996).
18. S. Veprek, M. Haussmann, S. Reiprich *et al*. *Surf. Coat. Technol*. **86–87**, 394 (1996).
19. A. A. Voevodin and J. S. Zabinski. *Thin Solid Films* **370**, 233 (2000).
20. P. Nesladek. Ph.D. Thesis, Technical University Munich (2000).
21. P. Karvankova, H. Männling, Ch. Eggs, S. Veprek. *Surf. Coat. Technol*. **146–147**, 146 (2001).

22. S. Veprek and A. S. Argon. *J. Vac. Sci. Technol. B* **20** (2002). In press.
23. R. A. Andrievski, I. A. Anisimova, V. P. Anisimov. *Thin Solid Films* **205**, 171 (1991).
24. R. A. Andrievski. *J. Solid State Chem*. **133**, 249 (1997); *J. Mater. Sci.* **32**, 4463 (1997).
25. A. Kelly and N. H. Macmillan. *Strong Solids*, Clarendon, Oxford (1986).
26. S. Veprek, A. Niederhofer, K. Moto, P. Nesladek, H. Männling, T. Bolom. *Mater. Res. Soc. Symp. Proc.* **581**, 321 (1999).